

Quantum Circuit Representation of Bosonic Matrix Functions

Minhyeok Kang,¹ Gwonhak Lee,¹ Youngrong Lim,² and Joonsuk Huh^{3, 4, *}

¹*SKKU Advanced Institute of Nanotechnology (SAINT),
Sungkyunkwan University, Suwon 16419, South Korea*

²*Department of Physics, Chungbuk National University, Cheongju, Chungbuk 28644, Korea*

³*Department of Chemistry, Yonsei University, Seoul 03722, Republic of Korea*

⁴*Department of Quantum Information, Yonsei University, Incheon 21983, Republic of Korea*

(Dated: February 3, 2026)

Bosonic counting problems can be framed as estimation tasks of matrix functions such as the permanent, hafnian, and loop-hafnian, depending on the underlying bosonic network. Remarkably, the same functions also arise in spin models, including the Ising and Heisenberg models, where distinct interaction structures correspond to different matrix functions. This correspondence has been used to establish the classical hardness of simulating interacting spin systems by relating their output distributions to #P-hard quantities. Previous works, however, have largely been restricted to bipartite spin interactions, where transition amplitudes, which provide the leading-order contribution to the output probabilities, are proportional to the permanent. In this work, we extend the Ising model construction to arbitrary interaction networks and show that transition amplitudes of the Ising Hamiltonian are proportional to the hafnian and the loop-hafnian. The loop-hafnian generalizes both the permanent and hafnian, but unlike these cases, loop-hafnian-based states require Dicke-like superpositions, making the design of corresponding quantum circuits non-trivial. Our results establish a unified framework linking bosonic networks of single photons and Gaussian states with quantum spin dynamics and matrix functions. This unification not only broadens the theoretical foundation of quantum circuit models but also highlights new, diverse, and classically intractable applications.

I. INTRODUCTION

Quantum computers are believed to outperform classical ones, and thus demonstrating quantum computational advantage is of great interest in quantum computing. A prominent approach is quantum sampling [1]: sampling from the output distributions generated by a quantum system, which is believed to be intractable for classical computation. Several quantum sampling models have been proposed and demonstrated, including boson sampling [2–9], Gaussian boson sampling [10–16], quantum spin models [17–19], instantaneous quantum polynomial-time circuits [20], and random circuit sampling [21, 22].

Boson sampling [2] is the first model whose hardness was rigorously analyzed within computational complexity theory. It considers a linear optical network in which each input mode is prepared in either a single-photon state or the vacuum state. The output probabilities are proportional to the squared matrix permanents of Gaussian submatrices of the interferometer unitary. Since computing the permanent is #P-hard [23], there is no efficient classical sampling algorithm for boson sampling; otherwise, the polynomial hierarchy (PH) would collapse to the third level by Toda’s theorem [24], which is contrary to the widespread belief that PH is infinite and does not collapse. Boson sampling has since been demonstrated at small scales [3–9].

Despite these successes, boson sampling faces obstacles to demonstrating quantum advantage. Large inter-

ferometers are required to reach the collision-free regime (one photon per output mode); otherwise, the relevant submatrices contain identical rows, and permanents become easier to compute. Moreover, nondeterministic photon sources, photon loss, and detector inefficiencies limit scalability [25, 26].

Gaussian boson sampling (GBS) [10, 11] is an alternative to boson sampling. GBS uses squeezed states instead of single-particle states in boson sampling, and the output probabilities are proportional to squared hafnians or loop-hafnians of submatrices set by interferometers, squeezing, and displacement parameters. Since the hafnian can reproduce the permanent by setting the particular matrix structure, GBS includes the argument of boson sampling. Moreover, unlike single-photon sources, squeezed states can be prepared deterministically. Gaussian boson sampling has been experimentally demonstrated in a variety of platforms [12–16], and has enabled a wide range of applications, including quantum chemistry [27–29] and graph-related problems [30–37]. However, the performance is limited by squeezing parameters, loss, and inefficiency [38, 39].

As another alternative, quantum sampling based on spin models has been proposed [17]. In a balanced bipartite Ising spin model of a $2N$ spin-1/2 system, the transition amplitude of the N th power of the Hamiltonian from the all-spin-down to the all-spin-up state is proportional to the permanent of a real $N \times N$ matrix, leading to output probabilities nearly proportional to squared permanents. Although Ref. [17] has only considered exact sampling in the Ising setting, Ref. [18] extended the analysis to broader classes of spin models and established

* joonsukhuh@yonsei.ac.kr

Correspondences between Matrix functions, Graphs, Bosonic networks, and Spin networks

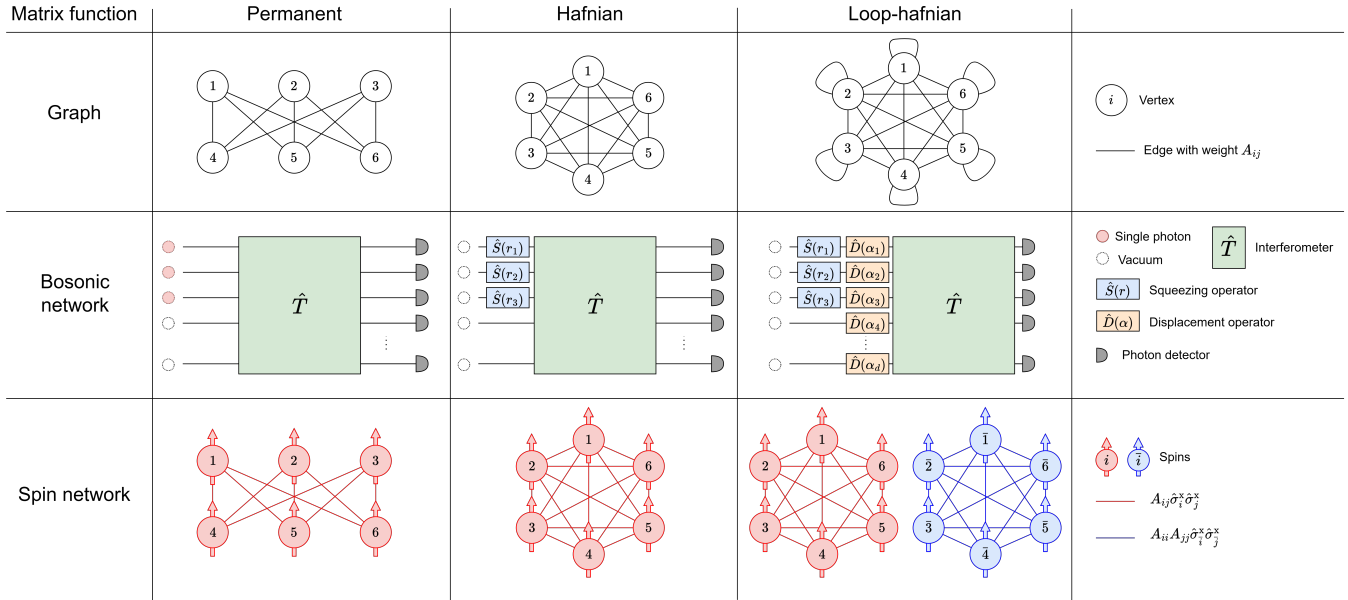


FIG. 1: Graphical summary of the correspondences between matrix functions, graph structures, bosonic networks, and spin networks. Each matrix function counts perfect matchings of a particular class of graphs. The matrix function depends on the input states in bosonic networks and on the interaction structure of spin networks. Note that the interaction structure of spin models for each matrix function is very similar to the corresponding class of graphs. For the permanent and hafnian cases, the spin network follows the graph exactly. In contrast, for the loop-hafnian case, the spin network consists of two connected components: one encoding edges between distinct vertices and the other encoding self-loops.

average-case hardness under the anticoncentration conjecture.

Compared to boson sampling, the spin model does not require the hiding property. Hence, the matrix is not limited to a random Gaussian matrix. The absence of the hiding property also implies that the collision-free condition, which is essential in boson sampling, is not required for the spin model. Thus the number of spins is thus smaller than the number of modes required in boson sampling. In addition, the initial state can be deterministically prepared.

Moreover, GBS relies on squeezing parameters, since they determine the matrix in the hafnian or loop-hafnian that governs the output probabilities. However, in the weak-squeezing regime, GBS becomes classically simulable, while generating strong squeezing parameters remains experimentally challenging. On the other hand, an arbitrary real symmetric matrix in the spin model can be encoded through interaction strengths.

Nonetheless, existing results of spin model have been limited to bipartite interactions, corresponding to the permanent. To explore more realistic architectures, it is necessary to generalize the interaction structure [10, 27, 31].

In this work, we extend the Ising spin model to arbitrary networks and show that the permanent, haf-

nian, and loop-hafnian can be represented in terms of their transition amplitudes. This representation provides a possibility to connecting quantum spin dynamics with complexity-theoretic hardness.

Our key observation is that the permanent in graph theory counts perfect matchings in bipartite graphs, which explains its appearance in bipartite spin models. We show that in arbitrary interacting Ising systems, the transition amplitude of the k th power of the Hamiltonian from the all-spin-down state to a configuration with $2k$ spin-ups is proportional to the hafnian of a $2k \times 2k$ submatrix, thereby generalizing the permanent.

Extending on this, we further construct the loop-hafnian case. Thus, our framework unifies permanents, hafnians, and loop-hafnians within spin dynamics. Notably, while the permanent and hafnian correspond to certain spin configurations, the loop-hafnian requires superpositions of states with fixed Hamming weight. Designing quantum circuits for such loop-hafnian states is non-trivial, as they rely on Dicke-like states, but they can, in principle, be realized on quantum computers. Therefore, our Ising spin model inherits the advantages of bipartite models and extends the interaction structure.

Fig. 1 shows the graphical summary of correspondences between matrix functions, graphs, bosonic networks, and spin networks. The matrix functions we consider count

perfect matchings of different graph structures, and the corresponding bosonic networks depend on their input states. Spin networks, on the other hand, depend on their interaction structures. For the simple graph cases, permanents and hafnians, the interaction structures resemble corresponding graphs, and matrix functions are related to certain spin configurations. The loop-hafnian case generalizes this picture to include self-loops: its interaction structure introduces an additional complete graph spin lattice associated with the self-loops, and the loop-hafnian corresponds to a superposition of spin configurations. Each matrix function thus reflects the combinatorial structure of the underlying quantum process.

This paper is organized as follows. In Sec. II, we introduce our quantum spin model and analyze its Hamiltonian. In Sec. III, we discuss the real symmetric matrices whose all diagonal elements are zero and their connection to hafnians and permanents. In Sec. IV, we extend the analysis to general real symmetric matrices for the loop-hafnian case. In Sec. V, we show how our framework unifies permanents, hafnians, and loop-hafnians. In Sec. VI, we discuss an efficient quantum circuit implementation. In particular, the quantum state required for the loop-hafnian case is nontrivial, we describe its preparation in Sec. VII. Finally, in Sec. VIII, we present our conclusion and discuss the future direction.

II. QUANTUM SPIN MODEL

Let $\mathbf{A} = [A_{ij}]$ be a real symmetric matrix of size $2N \times 2N$. We consider an Ising model without a transverse field, acting on a system of $4N$ spin-1/2 particles. The spin-up and spin-down states of a spin are denoted by $|\uparrow\rangle$ and $|\downarrow\rangle$, respectively. The corresponding Hamiltonian (see also Fig. 2) is given by:

$$\hat{H} = \frac{1}{2} \sum_{i \neq j}^{2N} (A_{ij} \hat{\sigma}_{x,i} \hat{\sigma}_{x,j} + A_{ii} A_{jj} \hat{\sigma}_{x,\bar{i}} \hat{\sigma}_{x,\bar{j}}), \quad (1)$$

where $\hat{\sigma}_{x,k}$ denotes the Pauli-X operator acting on the k th spin, and $\bar{k} = 2N + k$ for $k = 1, \dots, 2N$.

Since \hat{H} consists of products of Pauli-X operators $\hat{\sigma}_{x,i} \hat{\sigma}_{x,j}$ with $i \neq j$, each application of \hat{H} flips two spins, i.e., $\hat{\sigma}_{x,1} \hat{\sigma}_{x,2} |\uparrow\uparrow\rangle = |\downarrow\downarrow\rangle$. Thus, \hat{H}^k can flip at most $2k$ spins. Based on this logic, we show that the transition amplitude of the N th power of the Hamiltonian between two specific states, $|\phi_0\rangle$ and $|\phi_1\rangle$, is proportional to the loop-hafnian of \mathbf{A} , $\text{lhaf}(\mathbf{A})$ (see the definition in Eq. (20)).

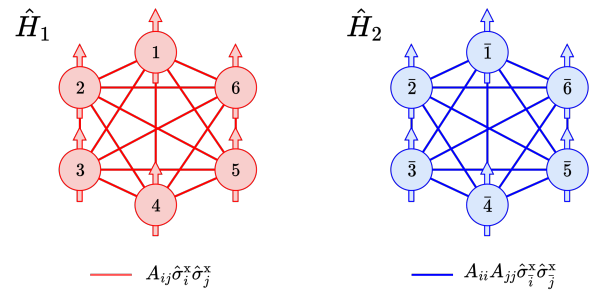


FIG. 2: Diagram of our quantum spin model with $2N = 6$. There are two connected components with the same number of spins generated by \hat{H}_1 (red) and \hat{H}_2 (blue), respectively.

We can decompose the Hamiltonian \hat{H} into two parts:

$$\hat{H} = \hat{H}_1 + \hat{H}_2, \quad (2)$$

$$\hat{H}_1 = \frac{1}{2} \sum_{i \neq j}^{2N} A_{ij} \hat{\sigma}_{x,i} \hat{\sigma}_{x,j}, \quad (3)$$

$$\hat{H}_2 = \frac{1}{2} \sum_{i \neq j}^{2N} A_{ii} A_{jj} \hat{\sigma}_{x,\bar{i}} \hat{\sigma}_{x,\bar{j}}. \quad (4)$$

Here, \hat{H}_1 and \hat{H}_2 act only on the first and last $2N$ spins, respectively. When all diagonal elements are zero ($A_{ii} = 0$ for all $i = 1, 2, \dots, N$), the system reduces to a simpler $2N$ spin model governed solely by the Hamiltonian \hat{H}_1 . We first discuss real symmetric matrices with zero diagonal elements, then extend this to generic real symmetric matrices.

Throughout this paper, we use the following notations to formalize our results. We define the index set $\mathcal{I} := \{1, 2, \dots, 2N\}$, and we denote the binomial coefficient as

$${}_n C_k = \binom{n}{k} = \frac{n!}{k!(n-k)!}. \quad (5)$$

For a $2N$ spin system, we define the state $|S\rangle$ for a subset $S \subset \mathcal{I}$ as the configuration where the spins indexed by S are up, while the other spins are down. For example, if $N = 2$ and $S = \{1, 3\}$, then $|S\rangle = |\uparrow\downarrow\uparrow\downarrow\rangle$. Note that $|\emptyset\rangle = |\downarrow\rangle^{\otimes 2N}$, where \emptyset denotes the empty set.

For a $4N$ -spin system, we write $|S, T\rangle = |S\rangle |T\rangle$ with $S, T \subset \mathcal{I}$. The states $|S\rangle$ and $|T\rangle$ are the quantum states for the first and the last $2N$ spins, respectively.

Given a real symmetric matrix $\mathbf{A} = [A_{ij}]$ of size $2N \times 2N$, we denote by $\mathbf{A}_S = [(A_S)_{ij}]$ the principal submatrix of \mathbf{A} induced by the subset $S \subset \mathcal{I}$. That is, \mathbf{A}_S consists of the rows and columns of \mathbf{A} corresponding to the indices in S . For example, if $N = 2$ and $S = \{1, 3\}$, then

$$\mathbf{A}_S = \begin{pmatrix} A_{11} & A_{13} \\ A_{31} & A_{33} \end{pmatrix}. \quad (6)$$

Finally, we adopt the convention that products of operators are ordered from right to left: $\prod_{i=1}^n \hat{A}_i = \hat{A}_n \cdots \hat{A}_2 \hat{A}_1$.

III. PERMANENTS AND HAFNIANS

We first consider the real symmetric matrix $\mathbf{A} = [A_{ij}]$ of size $2N \times 2N$, where all diagonal elements are zero: $A_{ii} = 0$ for all $i \in \mathcal{I}$. In this case, the Hamiltonian \hat{H} reduces to

$$\hat{H} = \hat{H}_1 = \frac{1}{2} \sum_{i \neq j}^{2N} A_{ij} \hat{\sigma}_{x,i} \hat{\sigma}_{x,j}. \quad (7)$$

Assume that the system is initialized in the spin-down state $|\emptyset\rangle = |\downarrow\rangle^{\otimes 2N}$. For $k \leq N$, the transition amplitude of \hat{H}^k between the states $|\emptyset\rangle$ and $|S\rangle$, where $S \subset \mathcal{I}$ and $|S| = 2k$ is given by

$$\langle S | \hat{H}^k | \emptyset \rangle = \begin{cases} k! \text{haf}(\mathbf{A}_S) & l = k, \\ 0 & \text{otherwise.} \end{cases} \quad (8)$$

Here, $\text{haf}(\mathbf{A}_S)$ is the hafnian of the matrix \mathbf{A}_S . Its derivation is detailed in Appendix A. The hafnian of a symmetric matrix $\mathbf{M} = [M_{ij}]$ of size $2n \times 2n$ is defined as

$$\text{haf}(\mathbf{M}) = \sum_{\rho \in P_{2n}^2} \prod_{\{i,j\} \in \rho} M_{ij}, \quad (9)$$

where P_{2n}^2 is the set of all partitions of the set $\{1, 2, \dots, 2n\}$ into subsets of size 2, e.g., $\{\{1, 2\}, \{3, 4\}, \{5, 6\}\} \in P_6^2$. In graph theory, $\text{haf}(\mathbf{M})$ is the sum of the products of the edge weights over all perfect matchings in a simple graph with the adjacency matrix \mathbf{M} .

Thus, the transition amplitude of \hat{H}^N between the states $|\phi_0\rangle = |\emptyset\rangle$ and $|\phi_1\rangle = |\mathcal{I}\rangle$ is given by

$$\langle \phi_1 | \hat{H}^N | \phi_0 \rangle = N! \text{haf}(\mathbf{A}). \quad (10)$$

When the $2N \times 2N$ real symmetric matrix \mathbf{A} has the form:

$$\mathbf{A} = \begin{pmatrix} \mathbf{O} & \mathbf{B} \\ \mathbf{B}^T & \mathbf{O} \end{pmatrix}, \quad (11)$$

where \mathbf{O} is the $N \times N$ zero matrix and $\mathbf{B} = [B_{ij}]$ is an $N \times N$ real matrix, the hafnian of \mathbf{A} equals the permanent of \mathbf{B} :

$$\text{haf}(\mathbf{A}) = \text{perm}(\mathbf{B}). \quad (12)$$

The permanent of \mathbf{B} is defined as

$$\text{perm}(\mathbf{B}) = \sum_{\sigma \in S_N} \prod_{i=1}^N B_{i\sigma(i)}, \quad (13)$$

where S_N is the symmetric group (the set of all permutations of $1, 2, \dots, N$). The form of the matrix in Eq. (11) can be interpreted as an adjacency matrix of the balanced bipartite graph with $2N$ vertices.

The corresponding Hamiltonian is constructed by partitioning $2N$ spins into two disjoint subsets of equal size (the first N spins and the last N spins, respectively) and including only interaction terms between the two subsets. It takes the form

$$\hat{H} = \sum_{i,j=1}^N B_{ij} \hat{\sigma}_{x,i} \hat{\sigma}_{x,N+j}. \quad (14)$$

This setting is identical to the model proposed in Refs. [17, 19]. The corresponding classical formula of Eq. (10), called the Glynn-Kan formula, was also proposed by Huh [19].

IV. LOOP-HAFNIANS

We now consider a general real symmetric matrix \mathbf{A} of size $2N \times 2N$, i.e., it may contain nonzero diagonal elements. In this case, the second term \hat{H}_2 must be included, and the full Hamiltonian is given by Eq. (1). Consequently, the system must involve $4N$ spins.

For a subset $S \subset \mathcal{I}$ of size $2k$ and its complement set S^c , the transition amplitude of \hat{H}^N between the states $|\emptyset, \emptyset\rangle$ and $|S, S^c\rangle$ is given by

$$\begin{aligned} \langle S, S^c | \hat{H}^N | \emptyset, \emptyset \rangle &= N!(2(N-k)-1)!! \left(\prod_{i \in S^c} A_{ii} \right) \text{haf}(\mathbf{A}_S). \end{aligned} \quad (15)$$

Its derivation is provided in Appendix B. Note that in the state $|S, S^c\rangle$, exactly $2N$ spins are up, and therefore $\langle S, S^c | \hat{H}^k | \emptyset, \emptyset \rangle = 0$ for $k < N$.

From Eq. (15), the value of the loop-hafnian of \mathbf{A} can be encoded in the transition amplitude of \hat{H}^N between the state $|\emptyset, \emptyset\rangle$ and an appropriate state. The loop-hafnian is a scalar function of a symmetric matrix. Loop-hafnian of a $n \times n$ real symmetric matrix $\mathbf{M} = [M_{ij}]$ is defined as

$$\text{lhaf}(\mathbf{M}) = \sum_{k=0}^n \sum_{\substack{S \subset \{1, \dots, n\} \\ |S|=k}} \left(\prod_{i \in S^c} M_{ii} \right) \text{haf}(\mathbf{M}_S). \quad (16)$$

In graph theory, $\text{lhaf}(\mathbf{M})$ is the sum of the products of edge weights over all perfect matchings in a loop-augmented graph with the adjacency matrix \mathbf{M} . In this interpretation, the diagonal entries of \mathbf{M} correspond to the weights of self-loops, while the off-diagonal elements represent the weights of edges between distinct vertices.

Thus using the relation between Eq. (15) and Eq. (16), and with $|\phi_0\rangle = |\emptyset, \emptyset\rangle$ and $|\phi_1\rangle$ defined as

$$|\phi_1\rangle = \frac{1}{\mathcal{L}_N} \sum_{k=0}^N \frac{1}{(2(N-k)-1)!!} \sum_{\substack{S \subset \mathcal{I} \\ |S|=2k}} |S, S^c\rangle \quad (17)$$

with the normalization factor \mathcal{L}_N defined as

$$\mathcal{L}_N^2 := \sum_{k=0}^N \frac{2^N C_{2k}}{[(2k-1)!!]^2}, \quad (18)$$

the transition amplitude of \hat{H}^N between $|\phi_0\rangle$ and $|\phi_1\rangle$ is

$$\langle \phi_1 | \hat{H}^N | \emptyset, \emptyset \rangle = \frac{N!}{\mathcal{L}_N} \text{lhaf}(\mathbf{A}). \quad (19)$$

Its derivation is detailed in Appendix C.

V. UNIFICATION OF PERMANENT, HAFNIAN AND LOOP-HAFNIAN

In Sec. III and Sec. IV, we showed how to encode the permanent, hafnian, and loop-hafnian in the transition amplitude of \hat{H}^N , and they can be unified into a single model.

While the form of permanent (Eq. (13)), hafnian (Eq. (9)), and loop-hafnian (Eq. (16)) seem different, they can be written as the loop-hafnian of matrices with different structures. Also, these structures of matrices are nested. For example, consider a $2N \times 2N$ real symmetric matrix \mathbf{A} . The loop-hafnian of \mathbf{A} is

$$\text{lhaf}(\mathbf{A}) = \sum_{k=0}^{2N} \sum_{\substack{S \subset \mathcal{I} \\ |S|=k}} \left(\prod_{i \in S} A_{ii} \right) \text{haf}(\mathbf{A}_S), \quad (20)$$

which is similar to the Laplace expansion of matrix permanents [40] (see also Ref. [41]). When all diagonal elements of \mathbf{A} are zero, only the $k=0$ term can be nonzero and thus Eq. (20) becomes the hafnian:

$$\text{lhaf}(\mathbf{A}) = \text{haf}(\mathbf{A}). \quad (21)$$

Also, if the \mathbf{A} has a form of Eq. (11), its diagonal elements are all zero, then by Eq. (12):

$$\text{lhaf}(\mathbf{A}) = \text{perm}(\mathbf{B}). \quad (22)$$

Therefore, permanent and hafnian can be integrated in the loop-hafnian, and the only difference is the structure of the matrices. It is natural because when we interpret the matrix \mathbf{A} as the adjacency matrix of a graph with $2N$ vertices, all these matrix functions can be expressed as sums over all perfect matchings in the graph, and the structure of the matrix represents the structure of the graph. Loop-hafnian, hafnian, and permanent are related to the loop-augmented graph, the simple graph, and the

balanced bipartite graph, respectively. These structures of graphs are nested, so are those of adjacency matrices. Therefore, all matrix functions can be encoded by using the model for the case in Sec. IV.

Moreover, we do not need to use the state $|\phi_1\rangle$ defined in Eq. (17), because not all diagonal elements need to be nonzero. Specifically, if there are p nonzero diagonal elements in the matrix \mathbf{A} , then we can set the state $|\phi_1\rangle$ as

$$|\phi_1\rangle = \frac{1}{\mathcal{L}_{N,\tilde{p}}} \sum_{k=N-\tilde{p}}^N \frac{1}{(2(N-k)-1)!!} \sum_{\substack{S \subset \mathcal{I} \\ |S|=2k}} |S, S^c\rangle \quad (23)$$

with $\tilde{p} = \lceil p/2 \rceil$, and the normalization factor $\mathcal{L}_{N,l}$ defined as

$$\mathcal{L}_{N,l}^2 := \sum_{k=0}^l \frac{2^N C_{2k}}{[(2k-1)!!]^2}. \quad (24)$$

Therefore, the transition amplitude of \hat{H}^N between $|\phi_0\rangle = |\emptyset, \emptyset\rangle$ and $|\phi_1\rangle$ is

$$\langle \phi_1 | \hat{H}^N | \phi_0 \rangle = \frac{N!}{\mathcal{L}_{N,\lceil p/2 \rceil}} \text{lhaf}(\mathbf{A}). \quad (25)$$

If all diagonal elements are zero, then $p=0$, therefore the state $|\phi_1\rangle = |\mathcal{I}, \emptyset\rangle$ and $\mathcal{L}_{N,0} = 1$. The transition amplitude becomes thus

$$\langle \phi_1 | \hat{H}^N | \phi_0 \rangle = N! \text{lhaf}(\mathbf{A}) = N! \text{haf}(\mathbf{A}), \quad (26)$$

which completely recovers the result of Eq. (10).

VI. QUANTUM SPIN DYNAMICS AND MATRIX FUNCTIONS

The quantum spin model we consider can be simulated on a circuit-based quantum computer with polynomial resources. Although we generally cannot implement N th power of \hat{H} on the quantum circuit directly [42], the transition overlap between two states $|\phi_0\rangle$ and $|\phi_1\rangle$ after a propagation time t approximately evaluates the transition amplitude of \hat{H}^N . The transition overlap is

$$\langle \phi_1 | e^{-i\hat{H}t} | \phi_0 \rangle = \sum_{n=0}^{\infty} \frac{(-it)^n}{n!} \langle \phi_1 | \hat{H}^n | \phi_0 \rangle \quad (27)$$

$$= \sum_{k=0}^{\infty} \frac{(-it)^{N+2k}}{(N+2k)!} \langle \phi_1 | \hat{H}^{N+2k} | \phi_0 \rangle \quad (28)$$

$$= \frac{(-it)^N}{\mathcal{L}_N} \text{lhaf}(\mathbf{A}) + \mathcal{O}(t^{N+2}). \quad (29)$$

Therefore, with a suitable choice of propagation time t as proposed in Ref. [17–19], we can estimate the loop-hafnian of \mathbf{A} with an additive error using, e.g., the Hadamard test. Moreover, calculating the permanent,

hafnian or the loop-hafnian is a $\#P$ -hard problem [43], the quantum spin model can be used for the sampling problem. On a quantum computer, each can represent a spin-1/2 particle with its states $|0\rangle$ and $|1\rangle$ by $|\uparrow\rangle$ and $|\downarrow\rangle$, respectively. Also, each Pauli- X gate \hat{X}_j can represent the Pauli operator of a spin $\hat{\sigma}_{x,j}$.

Since each Pauli term has forms of $\hat{\sigma}_{x,j}\hat{\sigma}_{x,k}$ and commutes with each other, the time evolution operator of the quantum spin model $\hat{U} = \exp(-i\hat{H}t)$ can be implemented by $\mathcal{O}(N^2)$ rotation- XX gates $\exp(-i\theta\hat{X}_j\hat{X}_k/2)$ without the Trotter error.

When all diagonal elements are zero, the two states $|\phi_0\rangle = |\emptyset\rangle$ and $|\phi_1\rangle = |\mathcal{I}\rangle$, which are encoded as $|0^{\otimes 2N}\rangle$ and $|1^{\otimes 2N}\rangle$, can be implemented straightforwardly. In the general case, the state $|\phi_1\rangle = |\emptyset, \emptyset\rangle$, encoded as $|0^{\otimes 4N}\rangle$, is also simple to realize. By contrast, the state $|\phi_1\rangle$ defined in Eq. (17) involves a superposition of configurations, making its implementation non-trivial. However, the encoded version of $|\phi_1\rangle$ can be prepared using $\mathcal{O}(N^2)$ controlled-NOT and single-qubit gates from $|0^{\otimes 4N}\rangle$, based on the implementation of Dicke state on the quantum computer [44]. Its implementation is detailed in the following section.

For simulation of the Hamiltonian \hat{H} , the required connectivity depends on the structure of the matrix \mathbf{A} . Nonzero off-diagonal element A_{ij} requires the connection between the i -th and j -th qubits, and the connection between the i -th qubits and j -th qubits is required for nonzero diagonal elements A_{ii} and A_{jj} . For the permanent, hafnian, and loop hafnian, connectivity requires at most a complete (N, N) balanced bipartite graph, $2N$ complete graph, and two $2N$ complete graphs, respectively. One of the suitable quantum computing platforms for simulating the quantum spin model we consider is a trapped-ion system, since any two qubits can be entangled [45–49] directly.

VII. PREPARATION OF $|\phi_1\rangle$ IN QUANTUM CIRCUIT

For the preparation of $|\phi_1\rangle$ in the circuit-based quantum computer from the state $|0^{\otimes 4N}\rangle$, we need to find an operator \hat{U} such that $|\phi_1\rangle = \hat{U}|0^{\otimes 4N}\rangle$.

Recall Eq. (17), now we treat the state $|\phi_1\rangle$ as the quantum state of qubit system ($|\downarrow\rangle$ and $|\uparrow\rangle$ are $|0\rangle$ and $|1\rangle$, respectively):

$$|\phi_1\rangle = \frac{1}{\mathcal{L}_N} \sum_{k=0}^N \frac{1}{[2(N-k)-1]!!} \sum_{\substack{S \in \mathcal{I} \\ |S|=2k}} |S, S^c\rangle. \quad (30)$$

Let $CX^{[i,j]}$ be the CNOT gate which the i th qubit is control and j th qubit is target. Then using CNOT gates,

two sets of $2N$ qubits can be disentangled:

$$\begin{aligned} & \prod_{i=1}^{2N} CX^{[i, \bar{i}]} |\phi_1\rangle := |\tilde{\psi}\rangle |1^{\otimes 2N}\rangle \\ &= \left(\frac{1}{\mathcal{L}_N} \sum_{k=0}^N \frac{1}{[2(N-k)-1]!!} \sum_{\substack{S \in \mathcal{I} \\ |S|=2k}} |S\rangle \right) |1^{\otimes 2N}\rangle. \end{aligned} \quad (31)$$

Now, what we need to prepare the state $|\tilde{\psi}\rangle$ in $2N$ qubit system. $|\tilde{\psi}\rangle$ can be rewritten as:

$$|\tilde{\psi}\rangle = \frac{1}{\mathcal{L}_N} \sum_{k=0}^N \frac{(2N C_{2k})^{1/2}}{[2(N-k)-1]!!} |D_{2k}^{2N}\rangle. \quad (32)$$

Here, $|D_{2k}^{2N}\rangle$ is a Dicke state, the equal amplitude superposition of basis states of $2N$ qubits with the same Hamming weight $2k$:

$$|D_{2k}^{2N}\rangle = \frac{1}{(2N C_{2k})^{1/2}} \sum_{\substack{S \in \mathcal{I} \\ |S|=2k}} |S\rangle. \quad (33)$$

Ref. [44] have suggested the unitary operator $\hat{U}_{2N,2N}$ which can prepare the Dicke state $|D_{2k}^{2N}\rangle$ from $|0^{\otimes 2(N-k)}\rangle |1^{\otimes 2k}\rangle$ for any $0 \leq k \leq N$. Since $U_{2N,2N}$ consists of $\mathcal{O}(4N^2)$ 2-qubit controlled rotation gates and CNOT gates, it can be implemented by $\mathcal{O}(4N^2)$ single and two-qubit gates. Thus,

$$\hat{U}_{2N,2N}^\dagger |\tilde{\psi}\rangle = \frac{1}{\mathcal{L}_N} \sum_{k=0}^N \frac{(2N C_{2k})^{1/2}}{[2(N-k)-1]!!} |0^{\otimes 2(N-k)}\rangle |1^{\otimes 2k}\rangle. \quad (34)$$

$\hat{U}_{2N,2N}^\dagger |\tilde{\psi}\rangle$ can be prepared by

$$\hat{U}_{2N,2N}^\dagger |\tilde{\psi}\rangle = \hat{V} |0^{\otimes 2N}\rangle, \quad (35)$$

where the operator \hat{V} is

$$\hat{V} = \prod_{m=0}^{N-1} CX^{[2N-2m, 2N-2m-1]} CR_y^{[2N+1-2m, 2N-2m]}(\theta_m), \quad (36)$$

where $CR_y^{[i,j]}(\theta) = |0\rangle\langle 0|_i \otimes \hat{I}_j + |1\rangle\langle 1|_i \otimes \hat{R}_{j,y}(\theta)$ is the controlled Y-rotation gate, $\hat{R}_{y,j}(\theta) = \exp(-i\theta\hat{Y}_j/2)$ (See Fig. 3 (a)). We use $CR_y^{[2N+1, 2N]}(\theta_0) = \hat{R}_{y,2N}(\theta_0)$ for consistency. The rotation angles θ_m are

$$\theta_m = 2 \arccos \left(\frac{(2N C_{2m})^{1/2}/[2(N-m)-1]!!}{\sqrt{\sum_{k=m}^N \frac{2N C_{2k}}{[(2(N-k)-1]!!]^2}}} \right). \quad (37)$$

The quantum circuit for preparing $|\phi_1\rangle$ is illustrated in Fig. 3 (b).

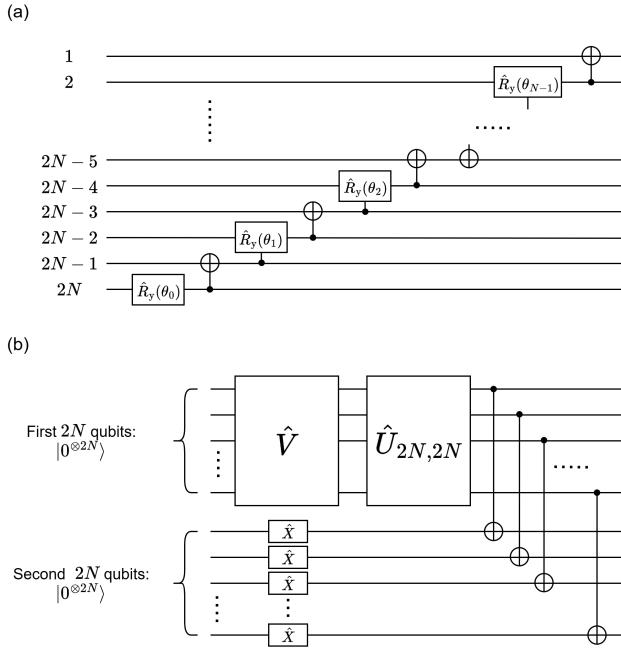


FIG. 3: (a) the quantum circuit for the operator \hat{V} . (b) the quantum circuit for preparing $|\phi_1\rangle$.

VIII. CONCLUSION AND DISCUSSION

In this work, we extended an Ising Hamiltonian from the bipartite spin construction to arbitrary interaction networks and showed that the permanents, hafnians, and loop-hafnians can be represented in terms of their transition amplitudes. This leads to a unified framework in which matrix functions emerge naturally from quantum spin dynamics. Moreover, we showed that such systems can be efficiently simulated on quantum hardware. Our results make it possible to broaden the known hardness of quantum spin models to arbitrary interaction structures.

Accordingly, the analysis of classical hardness remains an important direction for future work. Refs. [17, 18] considered classical hardness in bipartite Ising models. They used the fact that the transition amplitude is proportional to the permanent and provides the leading-order contribution to the output probability. In this work, our results show that a transition amplitude also can be proportional to the hafnian. Moreover, Eq. (8) implies that the transition amplitude also provides the leading-order contribution to the output probability. This contribution suggests that the output distributions over such configurations may exhibit classical hardness.

For the loop-hafnian case, the output states differ from those in the hafnian case. The output states giving transition amplitudes proportional to the loop-hafnian a submatrix are constructed by utilizing the state $|\phi_1\rangle$: for a subset $S \subset \mathcal{I}$, the qubits labeled by i and i for all $i \in S$ are collectively prepared in the state $|\phi_1\rangle$ with the corresponding subset size, while all remaining qubits are

kept in the $|\downarrow\rangle$ state. These states are superpositions of configurations of weight $2k$, making it difficult to distinguish the underlying contributions through simple measurement.

Nevertheless, these output states are mutually orthogonal. For any two distinct subsets $S, T \subset \mathcal{I}$, there exists an element $i \in S$ such that $i \notin T$. As a result, the spins i and \bar{i} are in different spin states in all configurations contributing to the output state associated with S , whereas the same spin pair is in the spin-down state in all configurations contributing to the output state associated with T , implying orthogonality. Hence, there exists a unitary \hat{U} that maps each such state to a trivial configuration of weight $2k$.

This observation enables a submatrix-sampling scheme in our commuting- XX spin circuits: prepare $|\phi_0\rangle$, evolve under $e^{-i\hat{H}t}$, postselect on a fixed Hamming-weight sector, apply \hat{U} , and sample outcomes labeled by $S \subset I$. In the hafnian case the leading-order transition amplitudes satisfy $\langle S | \hat{H}^k | \emptyset \rangle = k! \text{haf}(A_S)$, and in the loop-hafnian case the decoded amplitudes select $\text{lhaf}(A_S)$, so the within-fixed-weight output distribution is governed (to leading order in t) by $|\text{haf}(A_S)|^2$ or $|\text{lhaf}(A_S)|^2$, respectively.

Taken together, our results offer a way to extend the classical hardness frontier of spin-based quantum dynamics, unify the roles of permanents, hafnians, and loop-hafnians across bosonic networks and spin systems, and highlight several promising directions for future work. These include establishing rigorous hardness for hafnian (and loop-hafnian) sampling, and developing efficient quantum circuit designs for Dicke-like state preparation. Progress along these directions would deepen the complexity-theoretic foundations of quantum spin dynamics and strengthen its potential for demonstrating quantum advantage.

ACKNOWLEDGMENTS

This work was partly supported by the following multiple funding sources: [1] Basic Science Research Program through the National Research Foundation of Korea (NRF), funded by the Ministry of Science and ICT (RS-2023-NR068116, RS-2025-03532992). [2] Institute for Information & Communications Technology Promotion (IITP) grant funded by the Korea government (MSIP) (No. 2019-0-00003, No. RS-2024-00437284), which focuses on the research and development of core technologies for programming, running, implementing, and validating fault-tolerant quantum computing systems. [3] Yonsei University Research Fund under project number 2025-22-0140.

APPENDIX

Appendix A: Derivation of Eq. (8)

In this section, we show that $\langle S | \hat{H}^k | \emptyset \rangle = k! \text{haf}(\mathbf{A}_S)$ for all $S \subset \mathcal{I}$ such that $|S| = 2k$, for some $k \leq N$, using mathematical induction.

For $k = 1$, without loss of generality, assume that $S = \{1, 2\}$. then

$$\langle S | \hat{H} | \emptyset \rangle = \frac{1}{2} \sum_{i \neq j}^{2N} A_{ij} \langle S | \hat{\sigma}_i^x \hat{\sigma}_j^x | \emptyset \rangle = \frac{1}{2} \sum_{i \neq j}^{2N} A_{ij} \langle S | \{i, j\} \rangle \quad (\text{A1})$$

$$= \frac{1}{2} (A_{12} + A_{21}) = A_{12} = \text{haf}(\mathbf{A}_S). \quad (\text{A2})$$

Let assume there is some $k < N$ that satisfies $\langle S | \hat{H}^k | \emptyset \rangle = k! \text{haf}(\mathbf{A}_S)$ for all subset $S \subset \mathcal{I}$ such that $|S| = 2k$. Let $V \subset \mathcal{I}$ has $2(k+1) = 2k+2$ elements. Without loss of generality, we can choose $V = \{1, 2, \dots, 2k+1, 2k+2\}$. The Hafnian of \mathbf{A}_V can be written by the sum of hafnians of principal submatrices of A induced by subsets of V that has $2k$ elements:

$$\text{haf}(\mathbf{A}_V) = \frac{1}{k+1} \sum_{i < j}^{2k+2} A_{ij} \text{haf}(\mathbf{A}_{V-\{i,j\}}). \quad (\text{A3})$$

Here, $1/(k+1)$ is correction factor to eliminate the multiplicity. The transition amplitude of \hat{H}^{k+1} between $|\emptyset\rangle$ and $|V\rangle$ is

$$\langle V | \hat{H}^{k+1} | \emptyset \rangle = \langle V | \hat{H} \hat{H}^k | \emptyset \rangle \quad (\text{A4})$$

$$= \frac{1}{2} \sum_{i \neq j}^{2N} A_{ij} \langle V | \hat{\sigma}_i^x \hat{\sigma}_j^x \hat{H}^k | \emptyset \rangle \quad (\text{A5})$$

$$= \sum_{i < j}^{2N} A_{ij} \langle V | \hat{\sigma}_i^x \hat{\sigma}_j^x \hat{H}^k | \emptyset \rangle. \quad (\text{A6})$$

Since $V = \{1, 2, \dots, 2k+2\}$, the first $2k+2$ spins are up and the others are down in the state $|V\rangle$, thus $1 \leq i < j \leq 2k+2$ terms in RHS of Eq. (A4) only can be nonzero, otherwise $\hat{\sigma}_i^x \hat{\sigma}_j^x |V\rangle$ has $2k+2$ or $2k+4$ spin-ups, but \hat{H}^k flips at most $2k$ spins. Thus

$$\sum_{i < j}^{2N} A_{ij} \langle V | \hat{\sigma}_i^x \hat{\sigma}_j^x \hat{H}^k | \emptyset \rangle = \sum_{i < j}^{2k+2} A_{ij} \langle V - \{i, j\} | \hat{H}^k | \emptyset \rangle \quad (\text{A7})$$

$$= k! \sum_{i < j}^{2k+2} A_{ij} \text{haf}(\mathbf{A}_{V-\{i,j\}}) = (k+1)! \text{haf}(\mathbf{A}_V). \quad (\text{A8})$$

This result holds for arbitrary subset of \mathcal{I} that contains $2k+2$. Therefore, $\langle S | \hat{H}^k | \emptyset \rangle = k! \text{haf}(\mathbf{A}_S)$ holds for all $k \leq N$ and all subsets $S \subset \mathcal{I}$.

Appendix B: Derivation of Eq. (15)

Assume that a subset $S \subset \mathcal{I}$ has $2k$ elements: $|S| = 2k$. Since \hat{H}_1 commutes with \hat{H}_2 , the transition amplitude of \hat{H}^N between $|\emptyset, \emptyset\rangle$ and $|S, S^c\rangle$ is

$$\langle S, S^c | \hat{H}^N | \emptyset, \emptyset \rangle = \langle S, S^c | (\hat{H}_1 + \hat{H}_2)^N | \emptyset, \emptyset \rangle \quad (\text{B1})$$

$$= \sum_{j=0}^N {}_N C_j \langle S | \hat{H}_1^j | \emptyset \rangle \langle S^c | \hat{H}_2^{N-j} | \emptyset \rangle. \quad (\text{B2})$$

Since $|S| = 2k$ and $|S^c| = 2(N-k)$, only $j = k$ term in Eq. (B2) can be nonzero. Thus

$$\langle S, S^c | \hat{H}^N | \emptyset, \emptyset \rangle = {}_N C_k \langle S | \hat{H}_1^k | \emptyset \rangle \langle S^c | \hat{H}_2^{N-k} | \emptyset \rangle \quad (\text{B3})$$

$$= {}_N C_k k! \text{haf}(\mathbf{A}_S) \langle S^c | \hat{H}_2^{N-k} | \emptyset \rangle. \quad (\text{B4})$$

$k! \text{haf}(\mathbf{A}_S)$ came from Eq. (8). Since \hat{H}_2 has same structure with \hat{H}_1 , we can utilize the Eq. (8) for the transition amplitude of \hat{H}_2^{N-k} between $|\emptyset\rangle$ and $|S^c\rangle$: $\langle S^c | \hat{H}_2^{N-k} | \emptyset \rangle = (N-k)! \text{haf}(\mathbf{L}_{S^c})$, where $\mathbf{L} = [L_{ij}]$ is a real symmetric matrix of size $2N \times 2N$ such that $L_{ij} = A_{ii} A_{jj}$. From Eq. (9), the hafnian of $\mathbf{L}_{S^c} = [(L_{S^c})_{ij}]$ is

$$\text{haf}(\mathbf{L}_{S^c}) = \sum_{\rho \in P_{2(N-k)}^2} \prod_{\{i,j\} \in \rho} (L_{S^c})_{ij} \quad (\text{B5})$$

$$= [2(N-k) - 1]!! \prod_{i \in S^c} A_{ii}. \quad (\text{B6})$$

Here, the product of \mathbf{L}_{S^c} with all partition $\rho \in P_{2(N-k)}^2$ is same and equal to the product of all A_{ii} with $i \in S^c$, and multiplicity of the partition $\left| P_{2(N-k)}^2 \right|$ is $[2(N-k) - 1]!!$. Therefore,

$$\begin{aligned} \langle S, S^c | \hat{H}^N | \emptyset, \emptyset \rangle \\ = N! [2(N-k) - 1]!! \left(\prod_{i \in S^c} A_{ii} \right) \text{haf}(\mathbf{A}_S). \end{aligned} \quad (\text{B7})$$

Appendix C: Derivation of $|\phi_1\rangle$ for loop hafnian

Let $|\phi_0\rangle = |\emptyset, \emptyset\rangle$. We hope to find the quantum state $|\phi_1\rangle$ such that

$$\langle \phi_1 | \hat{H}^N | \phi_0 \rangle = N! \text{lhaf}(\mathbf{A}), \quad (\text{C1})$$

as we have shown in the case of the hafnian. From Eq. (B7),

$$\frac{\langle S, S^c | \hat{H}^N | \emptyset, \emptyset \rangle}{[2(N-k) - 1]!!} = N! \left(\prod_{i \in S^c} A_{ii} \right) \text{haf}(\mathbf{A}_S). \quad (\text{C2})$$

Now, consider the loop-hafnian of the matrix \mathbf{A} from Eq. (16)

$$\text{lhaf}(\mathbf{A}) = \sum_{k=0}^{2N} \sum_{\substack{S \subset \mathcal{I} \\ |S|=k}} \left(\prod_{i \in S^c} A_{ii} \right) \text{haf}(\mathbf{A}_S) \quad (\text{C3})$$

$$= \sum_{k=0}^N \sum_{\substack{S \subset \mathcal{I} \\ |S|=2k}} \left(\prod_{i \in S^c} A_{ii} \right) \text{haf}(\mathbf{A}_S), \quad (\text{C4})$$

since the only subsets S of even size can be nonzero. By connecting with Eq. (C2),

$$N! \text{lhaf}(\mathbf{A}) = \sum_{k=0}^N \sum_{\substack{S \subset \mathcal{I} \\ |S|=2k}} \frac{1}{[2(N-k)-1]!!} \langle S, S^c | \hat{H}^N | \emptyset, \emptyset \rangle. \quad (\text{C5})$$

Therefore, the quantum state $|\phi_1\rangle$ would be

$$|\phi_1\rangle = \sum_{k=0}^N \frac{1}{[2(N-k)-1]!!} \sum_{\substack{S \subset \mathcal{I} \\ |S|=2k}} |S, S^c\rangle. \quad (\text{C6})$$

However, $|\phi_1\rangle$ in Eq. (C6) is not normalized:

$$\langle \phi_1 | \phi_1 \rangle = \sum_{k=0}^N \frac{2N C_{2k}}{[2(N-k)-1]!!^2} \quad (\text{C7})$$

$$= \sum_{k=0}^N \frac{2N C_{2k}}{(2k-1)!!^2} := \mathcal{L}_N^2. \quad (\text{C8})$$

This result follows from the fact that the number of subsets of \mathcal{I} containing $2k$ elements is $2N C_{2k}$, and $2N C_{2k} = 2N C_{2(N-k)}$. We define the square root of this value as the normalization factor \mathcal{L}_N . Therefore, the normalized quantum state is

$$|\phi_1\rangle = \frac{1}{\mathcal{L}_N} \sum_{k=0}^N \frac{1}{[2(N-k)-1]!!} \sum_{\substack{S \subset \mathcal{I} \\ |S|=2k}} |S, S^c\rangle \quad (\text{C9})$$

and thus

$$\langle \phi_1 | \hat{H}^N | \phi_0 \rangle = \frac{N!}{\mathcal{L}_N} \text{lhaf}(\mathbf{A}). \quad (\text{C10})$$

[1] D. Hangleiter and J. Eisert, Computational advantage of quantum random sampling, *Rev. Mod. Phys.* **95**, 035001 (2023).

[2] S. Aaronson and A. Arkhipov, The computational complexity of linear optics, in *Proceedings of the Forty-Third Annual ACM Symposium on Theory of Computing*, STOC '11 (Association for Computing Machinery, New York, NY, USA, 2011) p. 333–342.

[3] M. A. Broome, A. Fedrizzi, S. Rahimi-Keshari, J. Dove, S. Aaronson, T. C. Ralph, and A. G. White, Photonic boson sampling in a tunable circuit, *Science* **339**, 794 (2013).

[4] J. B. Spring, B. J. Metcalf, P. C. Humphreys, W. S. Kolthammer, X.-M. Jin, M. Barbieri, A. Datta, N. Thomas-Peter, N. K. Langford, D. Kundys, J. C. Gates, B. J. Smith, P. G. R. Smith, and I. A. Walmsley, Boson sampling on a photonic chip, *Science* **339**, 798 (2013).

[5] M. Tillmann, B. Dakić, R. Heilmann, S. Nolte, A. Szameit, and P. Walther, Experimental boson sampling, *Nat. Photonics* **7**, 540 (2013).

[6] A. Crespi, R. Osellame, R. Ramponi, D. J. Brod, E. F. Galvão, N. Spagnolo, C. Vitelli, E. Maiorino, P. Mataloni, and F. Sciarrino, Integrated multimode interferometers with arbitrary designs for photonic boson sampling, *Nat. Photonics* **7**, 545 (2013).

[7] J. Carolan, C. Harrold, C. Sparrow, E. Martín-López, N. J. Russell, J. W. Silverstone, P. J. Shadbolt, N. Matsuda, M. Oguma, M. Itoh, G. D. Marshall, M. G. Thompson, J. C. F. Matthews, T. Hashimoto, J. L. O'Brien, and A. Laing, Universal linear optics, *Science* **349**, 711 (2015).

[8] H. Wang, Y. He, Y.-H. Li, Z.-E. Su, B. Li, H.-L. Huang, X. Ding, M.-C. Chen, C. Liu, J. Qin, J.-P. Li, Y.-M. He, C. Schneider, M. Kamp, C.-Z. Peng, S. Höfling, C.-Y. Lu, and J.-W. Pan, High-efficiency multiphoton boson sampling, *Nat. Photonics* **11**, 361 (2017).

[9] H. Wang, J. Qin, X. Ding, M.-C. Chen, S. Chen, X. You, Y.-M. He, X. Jiang, L. You, Z. Wang, C. Schneider, J. J. Renema, S. Höfling, C.-Y. Lu, and J.-W. Pan, Boson sampling with 20 input photons and a 60-mode interferometer in a 10^{14} -dimensional hilbert space, *Phys. Rev. Lett.* **123**, 250503 (2019).

[10] C. S. Hamilton, R. Kruse, L. Sansoni, S. Barkhofen, C. Silberhorn, and I. Jex, Gaussian boson sampling, *Phys. Rev. Lett.* **119**, 170501 (2017).

[11] N. Quesada, J. M. Arrazola, and N. Killoran, Gaussian boson sampling using threshold detectors, *Phys. Rev. A* **98**, 062322 (2018).

[12] H.-S. Zhong, H. Wang, Y.-H. Deng, M.-C. Chen, L.-C. Peng, Y.-H. Luo, J. Qin, D. Wu, X. Ding, Y. Hu, P. Hu, X.-Y. Yang, W.-J. Zhang, H. Li, Y. Li, X. Jiang, L. Gan, G. Yang, L. You, Z. Wang, L. Li, N.-L. Liu, C.-Y. Lu, and J.-W. Pan, Quantum computational advantage using photons, *Science* **370**, 1460 (2020).

[13] H.-S. Zhong, L.-C. Peng, Y. Li, Y. Hu, W. Li, J. Qin, D. Wu, W. Zhang, H. Li, L. Zhang, Z. Wang, L. You, X. Jiang, L. Li, N.-L. Liu, J. P. Dowling, C.-Y. Lu, and J.-W. Pan, Experimental gaussian boson sampling, *Sci. Bull.* **64**, 511 (2019).

[14] S. Paesani, Y. Ding, R. Santagati, L. Chakhmakhchyan, C. Vigliar, K. Rottwitt, L. K. Oxenløwe, J. Wang, M. G. Thompson, and A. Laing, Generation and sampling of quantum states of light in a silicon chip, *Nat. Phys.* **15**, 925 (2019).

[15] Y. Li, L. Gan, M. Chen, Y. Chen, H. Lu, C. Lu, J. Pan, H. Fu, and G. Yang, Benchmarking 50-photon gaussian boson sampling on the sunway taihulight, *IEEE Trans. Parallel Distrib. Syst.* **33**, 1357 (2022).

[16] J. M. Arrazola, V. Bergholm, K. Brádler, T. R. Bromley, M. J. Collins, I. Dhand, A. Fumagalli, T. Gerrits, A. Goussev, L. G. Helt, J. Hundal, T. Isacsson, R. B. Israel, J. Izaac, S. Jahangiri, R. Janik, N. Killoran, S. P. Kumar, J. Lavoie, A. E. Lita, D. H. Mahler, M. Menotti, B. Morrison, S. W. Nam, L. Neuhaus, H. Y. Qi, N. Quesada, A. Repington, K. K. Sabapathy, M. Schuld, D. Su, J. Swinarton, A. Száva, K. Tan, P. Tan, V. D. Vaidya, Z. Vernon, Z. Zabaneh, and Y. Zhang, Quantum circuits with many photons on a programmable nanophotonic chip, *Nature* **591**, 54 (2021).

[17] B. Fefferman, M. Foss-Feig, and A. V. Gorshkov, Exact sampling hardness of ising spin models, *Phys. Rev. A* **96**, 032324 (2017).

[18] C.-Y. Park, P. A. M. Casares, J. M. Arrazola, and J. Huh, The hardness of quantum spin dynamics (2023), arXiv:2312.07658 [quant-ph].

[19] J. Huh, Quantum estimation bound of the gaussian matrix permanent, *Phys. Rev. A* **111**, 012418 (2025).

[20] M. J. Bremner, A. Montanaro, and D. J. Shepherd, Average-case complexity versus approximate simulation of commuting quantum computations, *Phys. Rev. Lett.* **117**, 080501 (2016).

[21] S. Boixo, S. V. Isakov, V. N. Smelyanskiy, R. Babbush, N. Ding, Z. Jiang, M. J. Bremner, J. M. Martinis, and H. Neven, Characterizing quantum supremacy in near-term devices, *Nat. Phys.* **14**, 595 (2018).

[22] F. Arute, K. Arya, R. Babbush, D. Bacon, J. C. Bardin, R. Barends, R. Biswas, S. Boixo, F. G. S. L. Brandao, D. A. Buell, B. Burkett, Y. Chen, Z. Chen, B. Chiaro, R. Collins, W. Courtney, A. Dunsworth, E. Farhi, B. Foxen, A. Fowler, C. Gidney, M. Giustina, R. Graff, K. Guerin, S. Habegger, M. P. Harrigan, M. J. Hartmann, A. Ho, M. Hoffmann, T. Huang, T. S. Humble, S. V. Isakov, E. Jeffrey, Z. Jiang, D. Kafri, K. Kechedzhi, J. Kelly, P. V. Klimov, S. Knysh, A. Korotkov, F. Kostritsa, D. Landhuis, M. Lindmark, E. Lucero, D. Lyakh, S. Mandrà, J. R. McClean, M. McEwen, A. Megrant, X. Mi, K. Michielsen, M. Mohseni, J. Mutus, O. Naaman, M. Neeley, C. Neill, M. Y. Niu, E. Ostby, A. Petukhov, J. C. Platt, C. Quintana, E. G. Rieffel, P. Roushan, N. C. Rubin, D. Sank, K. J. Satzinger, V. Smelyanskiy, K. J. Sung, M. D. Treadthick, A. Vainsencher, B. Villalonga, T. White, Z. J. Yao, P. Yeh, A. Zalcman, H. Neven, and J. M. Martinis, Quantum supremacy using a programmable superconducting processor, *Nature* **574**, 505 (2019).

[23] L. Valiant, The complexity of computing the permanent, *Theor. Comput. Sci.* **8**, 189 (1979).

[24] S. Toda, Pp is as hard as the polynomial-time hierarchy, *SIAM J. Comput.* **20**, 865 (1991).

[25] S. Aaronson and D. J. Brod, Bosonsampling with lost photons, *Phys. Rev. A* **93**, 012335 (2016).

[26] R. García-Patrón, J. J. Renema, and V. Shchesnovich, Simulating boson sampling in lossy architectures, *Quantum* **3**, 169 (2019).

[27] J. Huh, G. G. Guerreschi, B. Peropadre, J. R. McClean, and A. Aspuru-Guzik, Boson sampling for molecular vibronic spectra, *Nat. Photonics* **9**, 615 (2015).

[28] Y. Shen, Y. Lu, K. Zhang, J. Zhang, S. Zhang, J. Huh, and K. Kim, Quantum optical emulation of molecular vibronic spectroscopy using a trapped-ion device, *Chem. Sci.* **9**, 836 (2018).

[29] C. S. Wang, J. C. Curtis, B. J. Lester, Y. Zhang, Y. Y. Gao, J. Freeze, V. S. Batista, P. H. Vaccaro, I. L. Chuang, L. Frunzio, L. Jiang, S. M. Girvin, and R. J. Schoelkopf, Efficient multiphoton sampling of molecular vibronic spectra on a superconducting bosonic processor, *Phys. Rev. X* **10**, 021060 (2020).

[30] K. Brádler, S. Friedland, J. Izaac, N. Killoran, and D. Su, Graph isomorphism and gaussian boson sampling, *Spec. Matrices* **9**, 166 (2021).

[31] L. Banchi, M. Fingerhuth, T. Babej, C. Ing, and J. M. Arrazola, Molecular docking with gaussian boson sampling, *Sci. Adv.* **6**, eaax1950 (2020).

[32] Y.-H. Deng, S.-Q. Gong, Y.-C. Gu, Z.-J. Zhang, H.-L. Liu, H. Su, H.-Y. Tang, J.-M. Xu, M.-H. Jia, M.-C. Chen, H.-S. Zhong, H. Wang, J. Yan, Y. Hu, J. Huang, W.-J. Zhang, H. Li, X. Jiang, L. You, Z. Wang, L. Li, N.-L. Liu, C.-Y. Lu, and J.-W. Pan, Solving graph problems using gaussian boson sampling, *Phys. Rev. Lett.* **130**, 190601 (2023).

[33] S. Yu, Z.-P. Zhong, Y. Fang, R. B. Patel, Q.-P. Li, W. Liu, Z. Li, L. Xu, S. Sagona-Stophel, E. Mer, S. E. Thomas, Y. Meng, Z.-P. Li, Y.-Z. Yang, Z.-A. Wang, N.-J. Guo, W.-H. Zhang, G. K. Tranmer, Y. Dong, Y.-T. Wang, J.-S. Tang, C.-F. Li, I. A. Walmsley, and G.-C. Guo, A universal programmable gaussian boson sampler for drug discovery, *Nat. Comput. Sci.* **3**, 839 (2023).

[34] J. M. Arrazola and T. R. Bromley, Using gaussian boson sampling to find dense subgraphs, *Phys. Rev. Lett.* **121**, 030503 (2018).

[35] J. M. Arrazola, T. R. Bromley, and P. Rebentrost, Quantum approximate optimization with gaussian boson sampling, *Phys. Rev. A* **98**, 012322 (2018).

[36] S. Sempere-Llagostera, R. B. Patel, I. A. Walmsley, and W. S. Kolthammer, Experimentally finding dense subgraphs using a time-bin encoded gaussian boson sampling device, *Phys. Rev. X* **12**, 031045 (2022).

[37] M. Schuld, K. Brádler, R. Israel, D. Su, and B. Gupt, Measuring the similarity of graphs with a gaussian boson sampler, *Phys. Rev. A* **101**, 032314 (2020).

[38] H. Qi, D. J. Brod, N. Quesada, and R. García-Patrón, Regimes of classical simulability for noisy gaussian boson sampling, *Phys. Rev. Lett.* **124**, 100502 (2020).

[39] N. Quesada and J. M. Arrazola, Exact simulation of gaussian boson sampling in polynomial space and exponential time, *Phys. Rev. Res.* **2**, 023005 (2020).

[40] P. Clifford and R. Clifford, The classical complexity of boson sampling, in *Proceedings of the Twenty-Ninth Annual ACM-SIAM Symposium on Discrete Algorithms* (SIAM, 2018) pp. 146–155.

[41] H. H. Zhu, H. Sen Chen, T. Chen, Y. Li, S. B. Luo, M. F. Karim, X. S. Luo, F. Gao, Q. Li, H. Cai, L. K. Chin, L. C. Kwek, B. Nordén, X. D. Zhang, and A. Q. Liu, Large-scale photonic network with squeezed vacuum states for molecular vibronic spectroscopy, *Nat. Commun.* **15**, 6057 (2024).

[42] J. C. Aulicino, T. Keen, and B. Peng, State preparation and evolution in quantum computing: A perspective from hamiltonian moments, *Int. J. Quantum Chem.* **122**, e26853 (2022).

- [43] A. Björklund, B. Gupt, and N. Quesada, A faster hafnian formula for complex matrices and its benchmarking on a supercomputer (2019).
- [44] A. Bärtschi and S. Eidenbenz, Deterministic preparation of dicke states, in *Fundamentals of Computation Theory*, edited by L. A. Gąsieniec, J. Jansson, and C. Levcopoulos (Springer International Publishing, Cham, 2019) pp. 126–139.
- [45] R. Blatt and C. F. Roos, Quantum simulations with trapped ions, *Nat. Phys.* **8**, 277 (2012).
- [46] C. Monroe, W. C. Campbell, L.-M. Duan, Z.-X. Gong, A. V. Gorshkov, P. W. Hess, R. Islam, K. Kim, N. M. Linke, G. Pagano, P. Richerme, C. Senko, and N. Y. Yao, Programmable quantum simulations of spin systems with trapped ions, *Rev. Mod. Phys.* **93**, 025001 (2021).
- [47] K. Wright, K. M. Beck, S. Debnath, J. M. Amini, Y. Nam, N. Grzesiak, J.-S. Chen, N. C. Pisenti, M. Chmielewski, C. Collins, K. M. Hudek, J. Mizrahi, J. D. Wong-Campos, S. Allen, J. Apisdorf, P. Solomon, M. Williams, A. M. Ducore, A. Blinov, S. M. Kreikemeier, V. Chaplin, M. Keesan, C. Monroe, and J. Kim, Benchmarking an 11-qubit quantum computer, *Nat. Commun.* **10**, 5464 (2019).
- [48] S. Debnath, N. M. Linke, C. Figgatt, K. A. Landsman, K. Wright, and C. Monroe, Demonstration of a small programmable quantum computer with atomic qubits, *Nature* **536**, 63 (2016).
- [49] M. Kang, W. Chen, H. Kwon, K. Kim, and J. Huh, Doubling Qubits in a Trapped-Ion System via Vibrational Dual-Rail Encoding, arXiv:2505.12937 (2025).